

Aligning Text to Image in Diffusion Models is Easier Than You Think

Jaa-Yeon Lee^{*1} Byunghee Cha^{*1} Jeongsol Kim² Jong Chul Ye¹

¹Kim Jaechul Graduate School of AI, KAIST

²Department of Bio and Brain Engineering, KAIST

{jaayeon, paulcha1025, jeongsol, jong.ye}@kaist.ac.kr

^{*}Equal contribution



Figure 1. **Representative results for image generation and image editing.** SoftREPA provides much improved text to image alignment by introducing a negligible size of learnable soft tokens.

Abstract

While recent advancements in generative modeling have significantly improved text-image alignment, some residual misalignment between text and image representations still remains. Although many approaches have attempted to address this issue by fine-tuning models using various reward models, etc., we revisit the challenge from the perspective

of representation alignment—an approach that has gained popularity with the success of REPresentation Alignment (REPA) [36]. We first argue that conventional text-to-image (T2I) diffusion models, typically trained on paired image and text data (i.e., positive pairs) by minimizing score matching or flow matching losses, is suboptimal from the standpoint of representation alignment. Instead, a better alignment can be achieved through contrastive learn-

ing that leverages both positive and negative pairs. To achieve this efficiently even with pretrained models, we introduce a lightweight contrastive fine-tuning strategy called *SoftREPA* that uses soft text tokens. This approach improves alignment with minimal computational overhead by adding fewer than 1M trainable parameters to the pretrained model. Our theoretical analysis demonstrates that our method explicitly increases the mutual information between text and image representations, leading to enhanced semantic consistency. Experimental results across text-to-image generation and text-guided image editing tasks validate the effectiveness of our approach in improving the semantic consistency of T2I generative models. Project Page: <https://softrepa.github.io/>

1. Introduction

Achieving effective alignment between modalities is essential in multimodal generative modeling. Specifically, latent diffusion models [26] enable various conditioning mechanisms, such as text, during the generation process for the semantic alignment between the two modalities.

For UNet-based denoisers [22, 24, 26], image representations are updated to align with fixed text representations encoded by pre-trained CLIP models through cross-attention layers. In contrast, transformer-based denoisers [7, 23] jointly update both text and image representations by concatenating them and processing them through self-attention layers. However, there is still room for further improvement, and to mitigate the remaining misalignment between text and image representations, a more effective representation learning approach is necessary.

Recent advancements in representation alignment for Diffusion Transformers (DiT) [23] have significantly enhanced their ability to learn semantically meaningful internal representations [9, 36]. Notably, REPA [36] demonstrated that aligning the internal representations of DiT with an external pre-trained visual encoder during training significantly improves both discriminative and generative performance.

To enhance the textual semantic alignment of DiT’s internal representations, we leverage these ideas to further enhance text-image alignment in text-to-image (T2I) generative models. Specifically, we are interested in the contrastive learning framework, a widely used strategy for multimodal alignment in most vision-language representation learning approaches such as CLIP [25], ALBEF [15], BLIP [16], ALIGN [10].

Most vision-language generative foundation models have focused on improving multimodal alignment through architectural modifications. These include MLP-based projection layers (e.g., LLaVA-style visual instruction tuning) [19, 20], cross-attention-based fusion mechanisms

(e.g., Flamingo, Stable Diffusion 1.5) [2, 22], and early fusion models that integrate text and vision features within a shared representation space (e.g., Chameleon, Stable Diffusion 3, FLUX) [7, 30]. In fact, many of these approaches have been largely adopted in T2I generative models. However, we explore an efficient yet effective way of further enhancing the representation alignment for given pre-trained models.

One of the most important contributions of this work is therefore the introduction of *soft text tokens* which are trained through contrastive text-and-image training. This allows the model to dynamically adapt its text representations, improving alignment with generated images without requiring full model finetuning. This simple yet effective approach significantly enhances text-to-image alignment in text-to-image generation and text-guided image editing tasks. Furthermore, the method is so flexible that it can be used with any pretrained T2I generative models. Theoretically, we show that this approach explicitly increases the mutual information between text and images, leading to better semantic consistency in multi-modal representations. We therefore refer to our method as *SoftREPA*, short for Soft REPresentation Alignment. Our contributions can be summarized as follows.

- We propose SoftREPA, a novel text-image representation alignment method that leverages a lightweight fine-tuning strategy with soft text tokens. This approach improves text-image alignment while adding fewer than 1M additional parameters, ensuring efficiency with minimal computational overhead.
- SoftREPA is simple yet flexible so that it can be used with any pretrained T2I generative models to improve performance of image generation, editing, etc.
- We show that our method explicitly increases mutual information between image and text, leading to better semantic consistency in multi-modal representations.

2. Preliminaries

Flow Models. Suppose that we have access to samples from target distribution $X_0 \sim q$ and source distribution $X_1 \sim p$. The goal of flow model is to generate X_0 starting from X_1 . Specifically, we define a velocity field $v_t(\mathbf{x})$ of a flow $\psi_t(\mathbf{x}) : [0, 1] \times \mathbb{R}^d \rightarrow \mathbb{R}^d$ that satisfies $\psi_t(X_0) = X_t$ and $\psi_1(X_0) = X_1$. Here, the ψ_t is uniquely characterized by a flow ODE:

$$d\psi_t(\mathbf{x}) = v_t(\psi_t(\mathbf{x}))dt \quad (1)$$

where the flow velocity v_t is fitted to the parameterized neural network $v_{t,\theta}$ via flow matching:

$$\mathcal{L}_{FM} = \mathbb{E}_{t \in [0,1], \mathbf{x}_t \sim p_t} \|v_t(\mathbf{x}_t) - v_{t,\theta}(\mathbf{x}_t)\|^2. \quad (2)$$

However, this is computationally expensive to solve due to the integration with respect to X_0 , so the authors in [18]

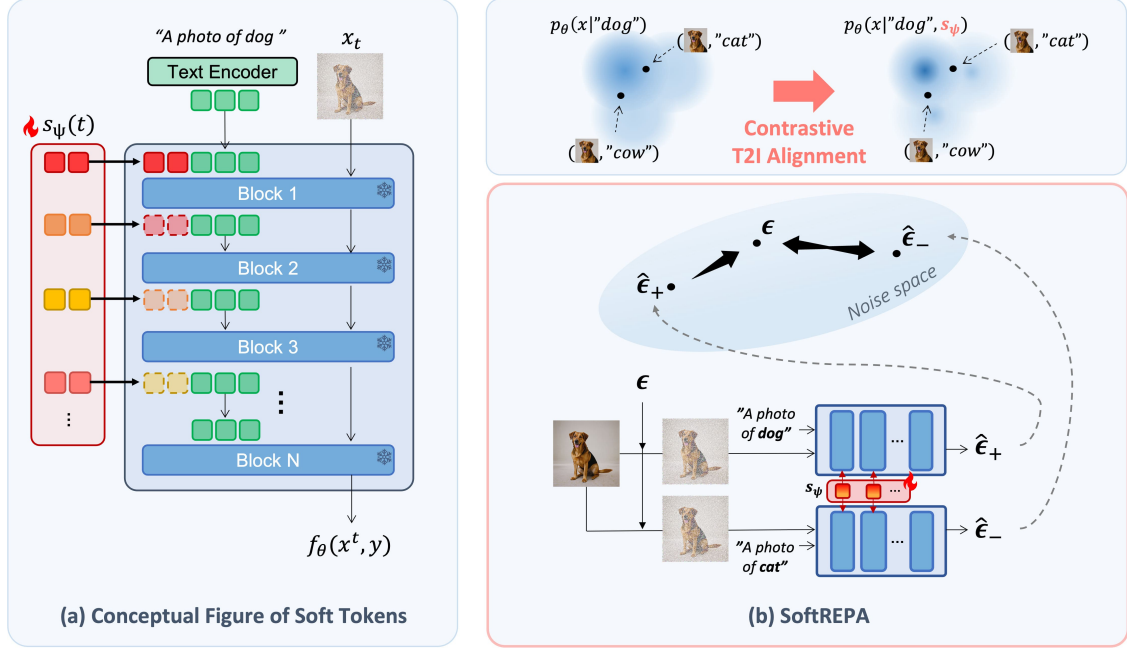


Figure 2. **Network architecture and algorithmic concept of SoftREPA.** (a) Learnable soft tokens are prepended to the text features across the upper layers, with each layer’s previous soft tokens being replaced by the soft tokens of the current layer. (b) The soft tokens are optimized to contrastively match the score with positively conditioned predicted noise while repelling the score from negatively conditioned predicted noise. This process implicitly sharpens the joint probability distribution of images and text by reducing the log probability of negatively paired conditions.

proposed a conditional flow matching that has the same gradient with the original objective function:

$$\mathcal{L}_{CFM} = \mathbb{E}_{t \in [0,1], x_0 \sim q} \|v_t(x_t|x_0) - v_{t,\theta}(x_t)\|^2, \quad (3)$$

where $v_t(x_t|x_0)$ is a conditional velocity field that defines a conditional flow $\psi_t(x_t|x_0)$ satisfying $\psi_t(x_1|x_0) = x_t$.

In particular, the linear conditional flow defines the flow as $x_t = \psi_t(x_1|x_0) = (1-t)x_0 + tx_1$. Then, we can compute the conditional velocity field $v_t(x_t|x_0) = \dot{\psi}_t(\psi_t^{-1}(x_t|x_0)|x_0) = x_1 - x_0$ [18]. Thus, the conditional flow matching loss is defined as

$$\mathbb{E}_{t \in [0,1], x_0, x_1 \sim \pi_{0,1}} \|(x_1 - x_0) - v_{t,\theta}(x_t)\|^2. \quad (4)$$

Considering a marginal velocity field,

$$\begin{aligned} v_t(x_t) &= \int v_t(x_t|x_0)p(x_0|x_t)dx_0 = \mathbb{E}[v_t(x_t|x_0)|x_t] \\ &= \mathbb{E}[x_1 - x_0|x_t] = \mathbb{E}[x_1|x_t] - \mathbb{E}[x_0|x_t], \end{aligned} \quad (5)$$

the generation process via flow ODE is

$$dx_t = v_t(x_t)dt = (\mathbb{E}[x_1|x_t] - \mathbb{E}[x_0|x_t])dt. \quad (6)$$

Accordingly,

$$\begin{aligned} dx_t &= \left(\mathbb{E} \left[\frac{x_t - (1-t)x_0}{t} | x_t \right] - \mathbb{E}[x_0|x_t] \right) dt \\ &= \frac{x_t - \mathbb{E}[x_0|x_t]}{t} dt \end{aligned} \quad (7)$$

which is the probability-flow ODE (PF-ODE) of DDIM [11, 28] when $x_1 \sim p := \mathcal{N}(0, \mathbf{I}_d)$. In other words, flow models and score-based models can be used interchangeably.

2.1. Contrastive Representation Learning

Contrastive learning aims to maximize the similarity between semantically related text-image pairs while pushing apart unrelated pairs in a shared representation space [5, 25]. Formally, given a batch of N image-text pairs $(\mathbf{I}_i, \mathbf{T}_i)_{i=1}^N$, contrastive learning optimizes a contrastive loss function, typically a variant of the InfoNCE loss:

$$\mathcal{L}_{\text{CLIP}} = -\frac{1}{N} \sum_{i=1}^N \log \frac{\exp(\text{sim}(\mathbf{I}_i, \mathbf{T}_i)/\tau)}{\sum_{j=1}^N \exp(\text{sim}(\mathbf{I}_i, \mathbf{T}_j)/\tau)} \quad (8)$$

where $\text{sim}(\mathbf{I}_i, \mathbf{T}_i)$ is a similarity metric such as cosine similarity or inner product between image and text embeddings, and τ denotes a temperature parameter that controls the distribution sharpness. This contrastive loss encourages image

and text representations to form a joint multimodal representation space, where aligned pairs are close together, and unaligned pairs are separated. Several fundamental models have successfully applied contrastive learning for multimodal representation learning [10, 15, 16, 25] and self-supervised learning [5].

Despite the success of contrastive learning in representation learning, its application in generative models remains underexplored due to key challenges. First, there is a fundamental mismatch between discriminative and generative features; conventional contrastive learning optimizes a representation space for discriminative tasks, whereas generative models focus on realistic sample synthesis. Second, text-image alignment in diffusion-based generative models is often implicit, relying on denoising objectives rather than explicit representation learning.

To bridge this gap, we propose a contrastive learning framework that aligns both representation learning and generative objectives, ensuring effective text-image representation alignment while preserving generative quality.

3. SoftREPA

3.1. Contrastive T2I Alignment Loss

Let $\{(\mathbf{x}^{(i)}, \mathbf{y}^{(i)})\}_{i=1}^n$ denotes the matched image and text pairs as a training data set. Then, contrastive text-to-image alignment in T2I model can be generally formulated as follows:

$$\mathcal{L} = -\frac{1}{n} \sum_{i=1}^n \log \frac{\exp(l(\mathbf{x}^{(i)}, \mathbf{y}^{(i)}))}{\sum_j \exp(l(\mathbf{x}^{(i)}, \mathbf{y}^{(j)}))} \quad (9)$$

where $l(\cdot, \cdot)$ represents the similarity measure. It is important to note that unlike the standard T2I model training that only consider positive pairs, i.e. $(\mathbf{x}^{(i)}, \mathbf{y}^{(i)})$, our SoftREPA employs the contrastive T2I alignment that additionally considers negative image and text pairs $(\mathbf{x}^{(i)}, \mathbf{y}^{(j)})$, $i \neq j$. This significantly improves the alignment performance.

Furthermore, in SoftREPA we define $l(\mathbf{x}^{(i)}, \mathbf{y}^{(j)})$ as the logit from the variation of the denoising score matching loss for the case of T2I diffusion models [31].

$$l(\mathbf{x}, \mathbf{y}) = e^{-\mathbb{E}_{t, \epsilon} [\|\epsilon_\theta(\mathbf{x}_t, t, \mathbf{y}) - \epsilon\|^2 / \tau(t)]} \quad (10)$$

Similarly, in conditional flow matching, the logit $l(\mathbf{x}, \mathbf{y})$ can be formalized as:

$$l(\mathbf{x}, \mathbf{y}) = e^{-\mathbb{E}_{t, \epsilon} [\|v_\theta(\mathbf{x}_t, t, \mathbf{y}) - (\epsilon - \mathbf{x}_0)\|^2 / \tau(t)]} \quad (11)$$

Here, $\tau(t)$ represents time scheduling parameter. One might consider using the denoising score matching loss, $-\mathbb{E}_{t, \epsilon} [\|\epsilon_\theta(\mathbf{x}_t, t, \mathbf{y}) - \epsilon\|^2]$, as a similarity measure instead of relying on its logit value. However, our experiments revealed that this formulation can introduce instability during

training due to the unbounded nature of the similarity measure. To address this, SoftREPA introduce an exponential function to constrain the logit values, effectively stabilizing the training process.

Intuitively, as illustrated in Fig. 2(b), training a diffusion model with this loss function would lead to predicted noise with matching text description align with the true noise. Conversely, when conditioned on a mismatched text, the predicted noise would deviate further from the true noise. It implies that the conditional probability distribution of the trained model gets sharpened, increasing the distinction between different text conditions, which is expected to enhance image-text alignment in the generated images.

3.2. The Soft Tokens

To distill the contrastive score matching objective above, we introduce a learnable soft token \mathbf{s}_ψ , which is the only trainable parameter while pretrained model remains frozen. In particular, as illustrated in Fig. 2, we introduce a set of learnable soft tokens that vary between layers and are indexed by time t . The soft token at layer k is defined using an embedding function with the number of soft tokens as m :

$$\mathbf{s}_\psi^{(k, t)} = \text{Embedding}(k, t) \in \mathbb{R}^{m \times d} \quad (12)$$

At the layer k , the text representation is updated by concatenating the time-indexed soft token with text hidden representation from the previous layer: $\hat{\mathbf{H}}_{\text{text}}^{(k-1, t)} = [\mathbf{s}_\psi^{(k, t)}; \mathbf{H}_{\text{text}}^{(k-1, t)}] \in \mathbb{R}^{(m+n) \times d}$.

The soft token is prepended on text features across the layers, leading to a modified denoising function: $v_\theta(\mathbf{x}_t, t, \mathbf{y}, \mathbf{s}_\psi)$. By adopting the soft tokens, we can adjust the image and text representations to get better semantic alignment. Additionally, for computational efficiency, we approximate the expectation within $l(\mathbf{x}, \mathbf{y})$ using a single Monte Carlo sample, effectively replacing it as

$$\tilde{l}(\mathbf{x}, \mathbf{y}, \mathbf{s}_\psi) = e^{-\|v_\theta(\mathbf{x}_t, t, \mathbf{y}, \mathbf{s}_\psi) - (\epsilon - \mathbf{x}_0)\|^2 / \tau(t)} \quad (13)$$

which can stabilize the computation using the same ϵ and t in the same batch. The resulting contrastive loss function with soft tokens can be defined as follows:

$$\mathcal{L}_{\text{SpfREPA}}(\psi) = -\mathbb{E}_{\substack{(\mathbf{x}, \mathbf{y}) \sim p_{\text{data}} \\ t \sim U(0, 1) \\ \epsilon \sim \mathcal{N}(\mathbf{0}, \mathbf{I})}} \log \frac{\exp(\tilde{l}(\mathbf{x}, \mathbf{y}, \mathbf{s}_\psi))}{\sum_j \exp(\tilde{l}(\mathbf{x}, \mathbf{y}^{(j)}, \mathbf{s}_\psi))} \quad (14)$$

Then the learnable token \mathbf{s}_ψ is optimized as follows:

$$\mathbf{s}_\psi^* = \arg \min_{\psi} \mathcal{L}_{\text{SpfREPA}}(\psi) \quad (15)$$

During inference, the trained soft tokens are leveraged with fixed text representation from the text encoder across layers and timesteps. The detailed procedure during the image generation process based on MM-DiT architecture is described in Algorithm 1.

Algorithm 1 Image Generation with Soft Tokens in MM-DiT

Require: Gaussian noise $\mathbf{z} \sim \mathcal{N}(\mathbf{0}, \mathbf{I})$
Require: Text $\mathbf{y} \sim p_{\text{data}}$
Require: Soft token $\mathbf{s}_\psi \sim \text{Embedding}(k, t)$
Require: Number of layers N , Threshold layer L
Require: Time steps $\{t_T, t_{T-1}, \dots, t_0\}$

- 1: Initialize $\mathbf{H}_{\text{img}}^{(0,T)} \leftarrow \mathbf{z}$
- 2: Initialize $\mathbf{H}_{\text{text}}^{(0,T)} \leftarrow \text{TextEncoder}(\mathbf{y})$
- 3: $n = \lfloor \mathbf{H}_{\text{text}}^{(0,T)} \rfloor$
- 4: **for** t in $\{t_T, t_{T-1}, \dots, t_0\}$ **do**
- 5: **for** $l = 1$ to N **do**
- 6: **if** $k \leq L$ **then**
- 7: $\mathbf{s}_\psi^{(k,t)} \leftarrow \text{Embedding}(k, t)$
- 8: $\hat{\mathbf{H}}_{\text{text}}^{(k-1,t)} \leftarrow [\mathbf{s}_\psi^{(k,t)}; \mathbf{H}_{\text{text}}^{(k-1,t)}]$
- 9: **else**
- 10: $\hat{\mathbf{H}}_{\text{text}}^{(k-1,t)} \leftarrow \mathbf{H}_{\text{text}}^{(k-1,t)}$
- 11: **end if**
- 12: $\mathbf{H}_{\text{img}}^{(k,t)}, \hat{\mathbf{H}}_{\text{text}}^{(k,t)} \leftarrow \text{Layer}_l(\mathbf{H}_{\text{img}}^{(k-1,t)}, \hat{\mathbf{H}}_{\text{text}}^{(k-1,t)})$
- 13: $\mathbf{H}_{\text{text}}^{(k,t)} \leftarrow \hat{\mathbf{H}}_{\text{text}}^{(k,t)}[-n :, :]$ \triangleright Drop soft tokens
- 14: **end for**
- 15: **end for**
- 16: **return** $\hat{\mathbf{X}} = \text{Decoder}(\mathbf{H}_{\text{img}}^{(N,t_0)})$

3.3. Relationship with Mutual Information

Although the relationship between contrastive loss and mutual information has been previously studied, we revisit it here to provide a more complete theoretical perspective. Additionally, we emphasize the critical role of the logit formulation in the score matching loss, highlighting its importance in ensuring stable and effective optimization.

According to [13], pointwise mutual information (PMI) over image \mathbf{x} and text \mathbf{y} pairs can be defined as follows:

$$i(\mathbf{x}, \mathbf{y}) = \log \frac{p_\theta(\mathbf{x}|\mathbf{y})}{p_\theta(\mathbf{x})} = \log \frac{p_\theta(\mathbf{x}|\mathbf{y})}{\mathbb{E}_{p(\mathbf{c})}[p_\theta(\mathbf{x}|\mathbf{c})]} \quad (16)$$

where the second equality follows from the definition of conditional expectation. Song et al. [29] and Kong et al. [13] further show that assuming the diffusion model is an optimal denoiser, the conditional likelihood $p_\theta(\mathbf{x}|\mathbf{y})$ can be described as (see Appendix A):

$$p_\theta(\mathbf{x}|\mathbf{y}) = \exp(\hat{l}(\mathbf{x}, \mathbf{y})), \quad (17)$$

where

$$\hat{l}(\mathbf{x}, \mathbf{y}) = -\frac{1}{2} \int_0^T \lambda(t) \mathbb{E}[\|\epsilon_\theta(\mathbf{x}_t, t, \mathbf{y}) - \epsilon\|^2] dt + C. \quad (18)$$

By approximating the denominator of PMI via Monte Carlo sampling, we arrive at:

$$i(\mathbf{x}, \mathbf{y}) \approx \log \frac{\exp(\hat{l}(\mathbf{x}, \mathbf{y}))}{\frac{1}{N} \sum_{\mathbf{c}} \exp(\hat{l}(\mathbf{x}, \mathbf{c}))} \quad (19)$$

This formulation closely resembles a cross-entropy loss, where the negative conditional log-likelihood $\hat{l}(\mathbf{x}, \mathbf{y})$ can be interpreted as logits.

From the fact that mutual information is the expectation of the pointwise mutual information, we derive:

$$I(X, Y) = \frac{1}{n} \sum_{i=1}^n \log \frac{\exp(\hat{l}(\mathbf{x}^{(i)}, \mathbf{y}^{(i)}))}{\sum_j \exp(\hat{l}(\mathbf{x}^{(i)}, \mathbf{y}^{(j)}))} + D \quad (20)$$

where $\mathbf{x}^{(i)}$ represents the i -th sample in the data, n denotes the number of samples in the data, and D indicates the constant.

Notably, Eq. (20) is very similar in form to the contrastive objective in Eq. (9), where the logit is the negative of the diffusion loss. This implies that minimizing our contrastive learning objective is closely related to maximizing the mutual information between image-text pairs under the diffusion model.

4. Experiments

Implementation details. In our experiments, to confirm the flexibility of SoftREPA, we utilize various open-source text-to-image diffusion models, including Stable Diffusion 1.5, Stable Diffusion XL, and Stable Diffusion 3 to evaluate text-to-image alignment in both image generation and editing tasks. The batch size was set to 16, and we trained the model for fewer than 30,000 iterations using two A100 GPUs.

For Stable Diffusion 3, we set the length of the soft token to 4 and used 5 layers to attach the soft tokens for further experiments. In the case of Stable Diffusion 1.5 and Stable Diffusion XL, the soft token length was set to 8, and soft tokens were applied only to the Down and Middle block layers of the UNet’s original embedding. Refer to further implementation detail in Appendix B.

Model	Human Preference	Text Alignment		Image Quality
	ImageReward \uparrow	CLIP \uparrow	HPS \uparrow	LPIPS \downarrow
SD1.5	0.177	0.265	0.251	0.438
SD1.5 (Ours)	0.274	0.271	0.252	0.437
SDXL	0.750	0.267	0.273	0.420
SDXL (Ours)	0.852	0.268	0.283	0.423
SD3	0.942	0.263	0.280	0.424
SD3 (Ours)	1.085	0.269	0.289	0.428

Table 1. Quantitative results of image generation regarding image quality and text alignment of generated images.

Text to Image Generation We conducted text-to-image generation experiments on SD1.5, SDXL, and SD3, training soft tokens using the text-image paired COCO dataset [17]. The implementation details are provided in Appendix B. To

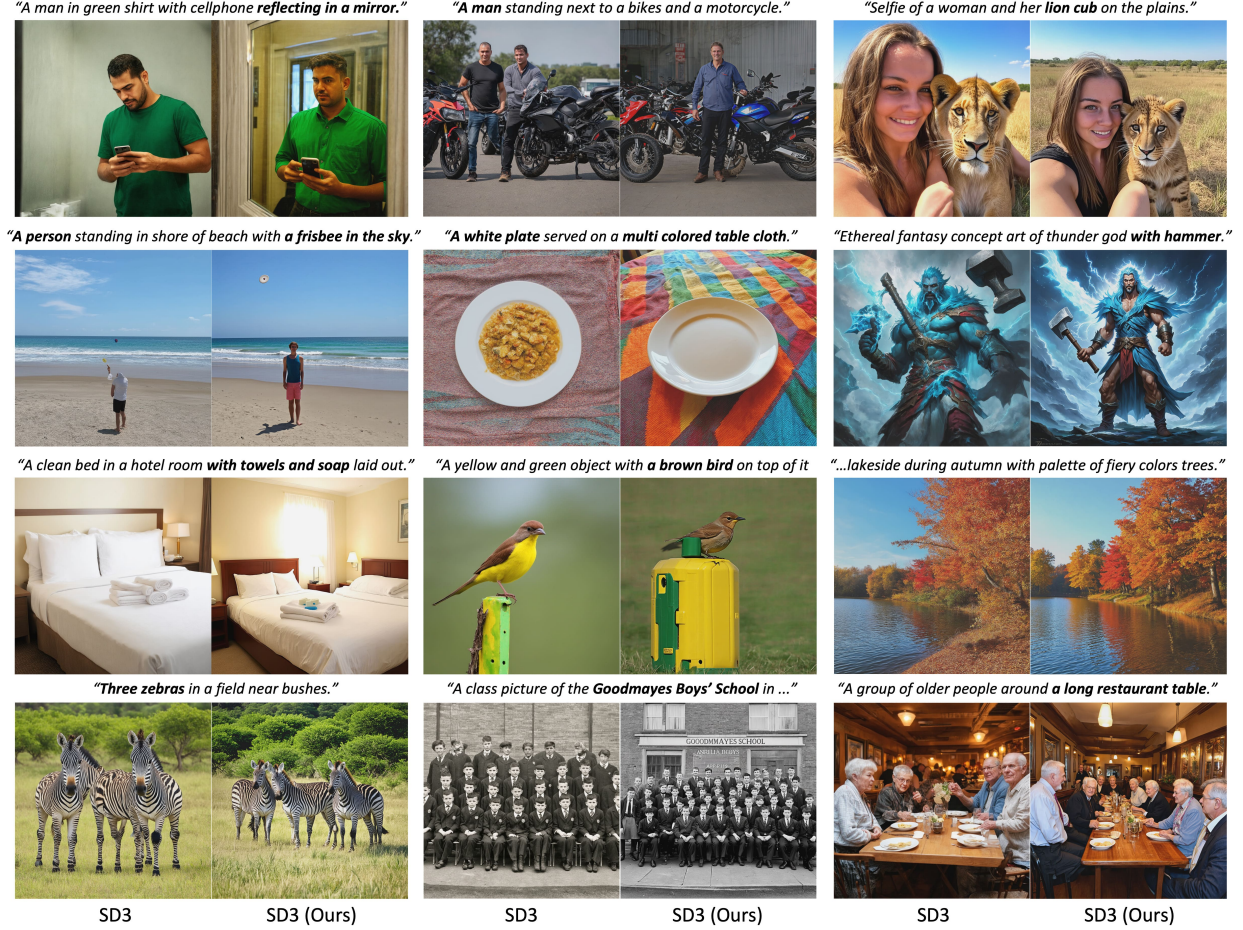


Figure 3. The qualitative results of text-to-image generation comparing SD3 and SD3 with proposed method. The given text is from COCO and Pixart dataset.

evaluate the generated images, we assessed human preference scores [12, 35], text-image alignment [34, 38], and image quality [27, 37]. As shown in Tab. 1, the proposed method generally outperforms baseline approaches in both diffusion and rectified flow model regardless of the model architecture. In particular, detailed textual descriptions are more accurately reflected in the generated images, as demonstrated in the qualitative results (Fig. 3).

Model	Dataset	Human Preference	Text Alignment		Image Quality
		ImageReward↑	CLIP↑	HPS↑	LPIPS↓
[14]	DIV2K	0.380	0.260	0.255	0.154
[14] (Ours)	DIV2K	0.466	0.263	0.260	0.149
[14]	Cat2Dog	0.937	0.225	0.266	0.199
[14] (Ours)	Cat2Dog	1.111	0.226	0.269	0.173

Table 2. Quantitative evaluation of image editing performance in terms of image quality and target text alignment. The editing process follows FlowEdit [14], with the only difference being the use of soft tokens.

Text Guided Image Editing To further demonstrate the improved text-image alignment achieved by our method, we conducted text-guided image editing experiments. These experiments are based on FlowEdit [14], an image editing framework for flow-matching models built on SD3. For the image editing dataset, we selected 800 high-quality images from the DIV2K dataset [1] and generated detailed captions for the source and target images using LLaVA [19]. The dataset generation process is described in detail in Appendix C.

According to FlowEdit [14], the optimal CFG scale for the target text condition is set to 13.5, with 33 editing steps out of 50 total timesteps. In contrast, with our proposed soft tokens, the CFG scale is reduced to 11, and the number of editing steps is reduced to 30, suggesting that our method could provide a more efficient way to capture the joint text-image distribution. In Fig. 4, the edits in both single and multi-concept scenarios are more effectively reflected in the modified images compared to vanilla SD3. Additional qual-

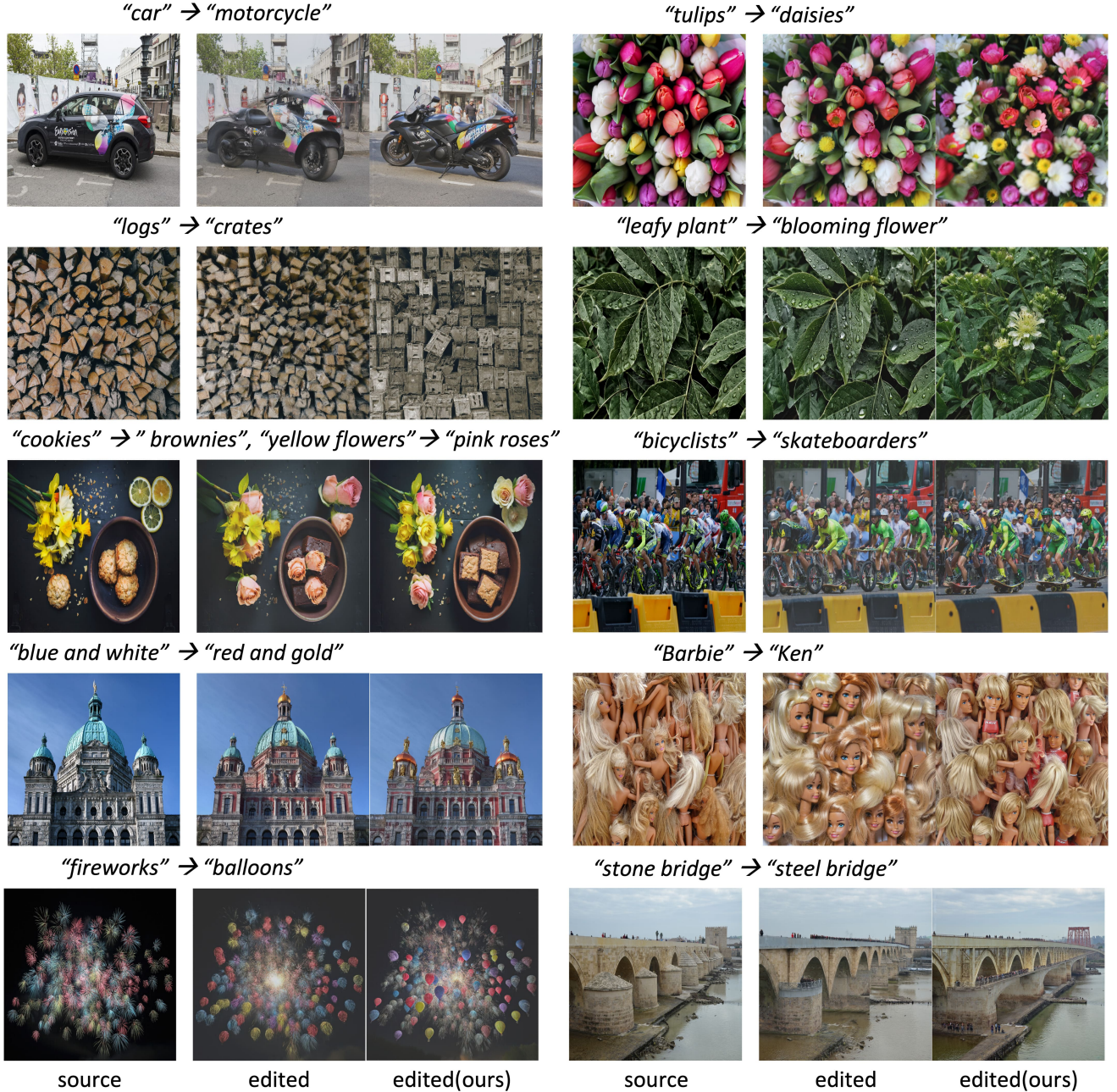


Figure 4. The qualitative results of text guided image editing comparing SD3 and SD3 with proposed method. The FlowEdit [14] is used as the editing method for both baseline and SoftREPA.

itative results are conducted on Cat2Dog dataset Fig. 6 with target CFG scale as 7.

Furthermore, the incorporation of soft tokens leads to improvements in both text-image alignment and overall image quality (Fig. 5). The quantitative results of human preference scores, text alignment, and perceptual image quality evaluation show consistent enhancements with the use of

soft tokens (Tab. 2). Detailed results for various parameter settings are provided in Appendix E.

Ablation Study We conducted an ablation study to assess the impact of both the number of layers incorporating soft text tokens and the length of these tokens on the text-to-image generation quality of SD3 using COCO val

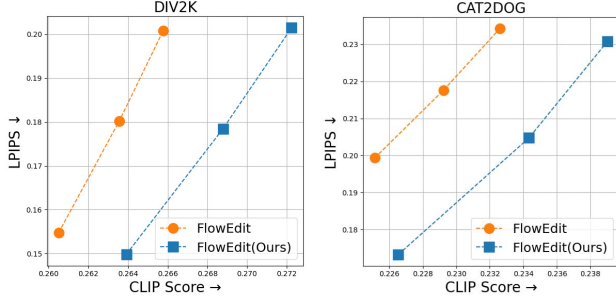


Figure 5. Quantitative comparisons between baseline editing and editing with soft tokens on DIV2K and Cat2Dog dataset. We evaluate CLIP score and LPIPS for each method. Lines connected with dots represent different CFG scales of the same method.



Figure 6. Additional qualitative results of text guided image editing on Cat2Dog dataset.

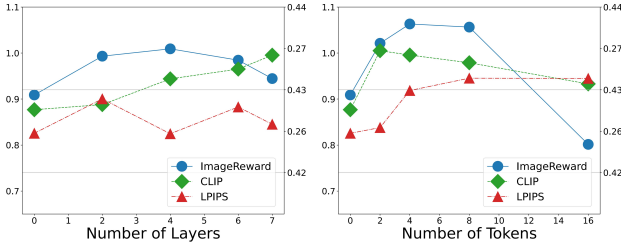


Figure 7. Ablation study analyzing the effect of the number of layers incorporating soft text tokens and the length of tokens. The evaluation is conducted using ImageReward, CLIP score and LPIPS. Each metric is normalized within its respective range: ImageReward [0.7, 1.1], CLIP score [0.25, 0.28], and LPIPS [0.42, 0.44].

dataset [17] (Fig. 7). A value of 0 corresponds to the vanilla SD3 model, and the number of layers is counted from the first layer. Each comparison is conducted with either a fixed token length of 8 or a fixed number of 5 layers. Our findings indicate that incorporating soft tokens beyond layer 7 severely degrades image generation quality. The optimal performance, aligned with human preferences (ImageRe-

ward [35]), was observed when soft tokens were applied within layers 2 ~ 5. This aligns with the model’s architectural design, where early layers primarily facilitate text-image alignment, while later layers focus on enhancing image fidelity [21]. However, text-image alignment scores (CLIP) continued to improve as more layers were tuned with soft tokens, which means that the model strongly follows the text conditions as more layers adopt the soft tokens while overall image quality remained stable across different layer configurations. The supporting qualitative results are presented in Appendix F.

Regarding token length, we found that using an excessive number of tokens, particularly beyond a length of 8, negatively impacted image generation quality. This suggests that longer token representations may lead to overfitting on the fine-tuning dataset (Fig. 7). Shorter token lengths (1 ~ 4 tokens) were beneficial for preserving perceptual similarity to the source dataset (LPIPS), whereas moderate token lengths (4 ~ 8 tokens) significantly enhanced text-image alignment, as indicated by CLIP scores and ImageReward. Qualitative results supporting these findings are presented in Appendix F.

5. Related Works

Several methods have been proposed to address the text-image misalignment. Training free approach such as CFG++ [6] addresses this problem as the off-manifold phenomenon of conventional CFG and reformulates it to a manifold-constrained CFG to get better text-to-image alignment. Other training-free approach, attend-and-excite [4], adjust attention activations to enhance text-image consistency. DOODL [32] applies guidance to end-to-end manner. Meanwhile, training-based approaches such as Diffusion-DPOK [33] introduce alignment losses during training to both enforce stronger text-conditioning and visual realism. Following Diffusion-DPO, denoising diffusion policy optimization(DDPO) [3] enhances the alignment using feedback from the pre-trained vision-language model. However, these methods require either extensive retraining or an additional human annotation dataset. In this paper, we use the prior knowledge of diffusion model itself to get better text and image alignment, proposing a novel SoftREPA on soft tokens.

6. Conclusion

In this work, we introduce SoftREPA, a novel approach for improving text-image alignment in generative models. Building on the success of prior representation alignment techniques, we extend the idea of internal representation alignment to the text-image alignment without relying on external encoders. Our method effectively integrates contrastive learning and score matching loss to enhance text-

image representation learning while preserving the generative capabilities of diffusion models. Also, we introduced soft text tokens, which can effectively adjust the image-text representations through contrastive T2I alignment, making it lightweight and efficient. We demonstrate that our approach enhances text-image alignment in both image generation and editing tasks while maintaining a minimal parameter overhead. Our experiments span various models, including Stable Diffusion 1.5, XL, and 3.

References

- [1] Eirikur Agustsson and Radu Timofte. Ntire 2017 challenge on single image super-resolution: Dataset and study. In *Proceedings of the IEEE conference on computer vision and pattern recognition workshops*, pages 126–135, 2017. 6
- [2] Jean-Baptiste Alayrac, Jeff Donahue, Pauline Luc, Antoine Miech, Iain Barr, Yana Hasson, Karel Lenc, Arthur Mensch, Katherine Millican, Malcolm Reynolds, et al. Flamingo: a visual language model for few-shot learning. *Advances in neural information processing systems*, 35:23716–23736, 2022. 2
- [3] Kevin Black, Michael Janner, Yilun Du, Ilya Kostrikov, and Sergey Levine. Training diffusion models with reinforcement learning. In *International Conference on Learning Representations*, 2024. 8
- [4] Hila Chefer, Yuval Alaluf, Yael Vinker, Lior Wolf, and Daniel Cohen-Or. Attend-and-excite: Attention-based semantic guidance for text-to-image diffusion models. *ACM transactions on Graphics (TOG)*, 42(4):1–10, 2023. 8
- [5] Ting Chen, Simon Kornblith, Mohammad Norouzi, and Geoffrey Hinton. A simple framework for contrastive learning of visual representations. *arXiv preprint arXiv:2002.05709*, 2020. 3, 4
- [6] Hyungjin Chung, Jeongsol Kim, Geon Yeong Park, Hyelin Nam, and Jong Chul Ye. Cfg++: Manifold-constrained classifier free guidance for diffusion models. *arXiv preprint arXiv:2406.08070*, 2024. 8
- [7] Patrick Esser, Sumith Kulal, Andreas Blattmann, Rahim Entezari, Jonas Müller, Harry Saini, Yam Levi, Dominik Lorenz, Axel Sauer, Frederic Boesel, et al. Scaling rectified flow transformers for high-resolution image synthesis. In *Forty-first international conference on machine learning*, 2024. 2
- [8] Aaron Grattafiori, Abhimanyu Dubey, Abhinav Jauhri, Abhinav Pandey, Abhishek Kadian, Ahmad Al-Dahle, Aiesha Letman, Akhil Mathur, Alan Schelten, Alex Vaughan, et al. The llama 3 herd of models. *arXiv preprint arXiv:2407.21783*, 2024. 11
- [9] Hyeonho Jeong, Chun-Hao Paul Huang, Jong Chul Ye, Niloy Mitra, and Duygu Ceylan. Track4gen: Teaching video diffusion models to track points improves video generation. *arXiv preprint arXiv:2412.06016*, 2024. 2
- [10] Chao Jia, Yinfei Yang, Ye Xia, Yi-Ting Chen, Zarana Parekh, Hieu Pham, Quoc Le, Yun-Hsuan Sung, Zhen Li, and Tom Duerig. Scaling up visual and vision-language representation learning with noisy text supervision. In *International conference on machine learning*, pages 4904–4916. PMLR, 2021. 2, 4
- [11] Tero Karras, Miika Aittala, Timo Aila, and Samuli Laine. Elucidating the design space of diffusion-based generative models. In *Proc. NeurIPS*, 2022. 3
- [12] Yuval Kirstain, Adam Polyak, Uriel Singer, Shihabuddin Matiana, Joe Penna, and Omer Levy. Pick-a-pic: An open dataset of user preferences for text-to-image generation. 2023. 6
- [13] Xianghao Kong, Ollie Liu, Han Li, Dani Yogatama, and Greg Ver Steeg. Interpretable diffusion via information decomposition. *arXiv preprint arXiv:2310.07972*, 2023. 5, 11
- [14] Vladimir Kulikov, Matan Kleiner, Inbar Huberman-Spiegelglas, and Tomer Michaeli. Flowedit: Inversion-free text-based editing using pre-trained flow models. *arXiv preprint arXiv:2412.08629*, 2024. 6, 7
- [15] Junnan Li, Ramprasaath Selvaraju, Akhilesh Gotmare, Shafiq Joty, Caiming Xiong, and Steven Chu Hong Hoi. Align before fuse: Vision and language representation learning with momentum distillation. *Advances in neural information processing systems*, 34:9694–9705, 2021. 2, 4
- [16] Junnan Li, Dongxu Li, Caiming Xiong, and Steven Hoi. Blip: Bootstrapping language-image pre-training for unified vision-language understanding and generation. In *International conference on machine learning*, pages 12888–12900. PMLR, 2022. 2, 4
- [17] Tsung-Yi Lin, Michael Maire, Serge Belongie, James Hays, Pietro Perona, Deva Ramanan, Piotr Dollár, and C Lawrence Zitnick. Microsoft coco: Common objects in context. In *Computer Vision—ECCV 2014: 13th European Conference, Zurich, Switzerland, September 6-12, 2014, Proceedings, Part V 13*, pages 740–755. Springer, 2014. 5, 8
- [18] Yaron Lipman, Ricky T. Q. Chen, Heli Ben-Hamu, Maximilian Nickel, and Matthew Le. Flow matching for generative modeling. In *The Eleventh International Conference on Learning Representations*, 2023. 2, 3
- [19] Haotian Liu, Chunyuan Li, Qingyang Wu, and Yong Jae Lee. Visual instruction tuning. *Advances in neural information processing systems*, 36:34892–34916, 2023. 2, 6, 11
- [20] Haotian Liu, Chunyuan Li, Yuheng Li, Bo Li, Yuanhan Zhang, Sheng Shen, and Yong Jae Lee. Llava-next: Improved reasoning, ocr, and world knowledge, 2024. 2
- [21] Benyuan Meng, Qianqian Xu, Zitai Wang, Xiaochun Cao, and Qingming Huang. Not all diffusion model activations have been evaluated as discriminative features. *Advances in Neural Information Processing Systems*, 37:55141–55177, 2025. 8
- [22] Suraj Patil, Pedro Cuenca, Nathan Lambert, and Patrick von Platen. Stable diffusion with diffusers. *Hugging Face Blog*, 2022. <https://huggingface.co/blog/stable-diffusion>. 2
- [23] William Peebles and Saining Xie. Scalable diffusion models with transformers. In *Proceedings of the IEEE/CVF international conference on computer vision*, pages 4195–4205, 2023. 2
- [24] Dustin Podell, Zion English, Kyle Lacey, Andreas Blattmann, Tim Dockhorn, Jonas Müller, Joe Penna, and

- Robin Rombach. Sdxl: Improving latent diffusion models for high-resolution image synthesis. *arXiv preprint arXiv:2307.01952*, 2023. 2
- [25] Alec Radford, Jong Wook Kim, Chris Hallacy, Aditya Ramesh, Gabriel Goh, Sandhini Agarwal, Girish Sastry, Amanda Askell, Pamela Mishkin, Jack Clark, et al. Learning transferable visual models from natural language supervision. In *International conference on machine learning*, pages 8748–8763. PmLR, 2021. 2, 3, 4
- [26] Robin Rombach, Andreas Blattmann, Dominik Lorenz, Patrick Esser, and Björn Ommer. High-resolution image synthesis with latent diffusion models. In *Proceedings of the IEEE/CVF Conference on Computer Vision and Pattern Recognition*, pages 10684–10695, 2022. 2
- [27] Maximilian Seitzer. pytorch-fid: FID Score for PyTorch. <https://github.com/mseitzer/pytorch-fid>, 2020. Version 0.3.0. 6
- [28] Jiaming Song, Chenlin Meng, and Stefano Ermon. Denoising diffusion implicit models. In *International Conference on Learning Representations*, 2021. 3
- [29] Yang Song, Conor Durkan, Iain Murray, and Stefano Ermon. Maximum likelihood training of score-based diffusion models. *Advances in Neural Information Processing Systems*, 34, 2021. 5, 11
- [30] Chameleon Team. Chameleon: Mixed-modal early-fusion foundation models. *arXiv preprint arXiv:2405.09818*, 2024. 2
- [31] Pascal Vincent. A connection between score matching and denoising autoencoders. *Neural computation*, 23(7):1661–1674, 2011. 4
- [32] Bram Wallace, Akash Gokul, Stefano Ermon, and Nikhil Naik. End-to-end diffusion latent optimization improves classifier guidance. In *ICCV*, 2023. 8
- [33] Bram Wallace, Meihua Dang, Rafael Rafailov, Linqi Zhou, Aaron Lou, Senthil Purushwalkam, Stefano Ermon, Caiming Xiong, Shafiq Joty, and Nikhil Naik. Diffusion model alignment using direct preference optimization. In *Proceedings of the IEEE/CVF Conference on Computer Vision and Pattern Recognition*, pages 8228–8238, 2024. 8
- [34] Xiaoshi Wu, Yiming Hao, Keqiang Sun, Yixiong Chen, Feng Zhu, Rui Zhao, and Hongsheng Li. Human preference score v2: A solid benchmark for evaluating human preferences of text-to-image synthesis. *arXiv preprint arXiv:2306.09341*, 2023. 6
- [35] Jiazheng Xu, Xiao Liu, Yuchen Wu, Yuxuan Tong, Qinkai Li, Ming Ding, Jie Tang, and Yuxiao Dong. Imagereward: learning and evaluating human preferences for text-to-image generation. In *Proceedings of the 37th International Conference on Neural Information Processing Systems*, pages 15903–15935, 2023. 6, 8
- [36] Sihyun Yu, Sangkyung Kwak, Huiwon Jang, Jongheon Jeong, Jonathan Huang, Jinwoo Shin, and Saining Xie. Representation alignment for generation: Training diffusion transformers is easier than you think. In *International Conference on Learning Representations*, 2025. 1, 2
- [37] Richard Zhang, Phillip Isola, Alexei A Efros, Eli Shechtman, and Oliver Wang. The unreasonable effectiveness of deep features as a perceptual metric. In *CVPR*, 2018. 6
- [38] SUN Zhengwentai. clip-score: CLIP Score for PyTorch. <https://github.com/taited/clip-score>, 2023. Version 0.1.1. 6

SoftREPA for better Text-to-Image Alignment

Supplementary Materials

A. Information Theory on Diffusion Model

Several studies have explored diffusion models from an information-theoretic viewpoint. According to [13], the mutual information between random variables X and Y can be expressed as the expectation of pointwise mutual information over their joint distribution:

$$I(X, Y) = \mathbb{E}_{p(\mathbf{x}, \mathbf{y})}[i(\mathbf{x}, \mathbf{y})], \quad (21)$$

where the pointwise mutual information (PMI) is defined as the difference between the conditional and marginal log-likelihoods of a given sample \mathbf{x} :

$$i(\mathbf{x}, \mathbf{y}) = \log p(\mathbf{x}|\mathbf{y}) - \log p(\mathbf{x}). \quad (22)$$

This quantity measures how much the presence of condition \mathbf{y} affects the probability distribution near \mathbf{x} .

Song et al. [29] and Kong et al. [13] showed that, under the assumption of an optimal diffusion model trained on given data, the log-likelihood of an image \mathbf{x} can be formulated as:

$$-\log p(\mathbf{x}) = \frac{1}{2} \int_0^T \lambda(t) \mathbb{E}_{t, \epsilon} [\|\epsilon_\theta(\mathbf{x}_t, t) - \epsilon\|^2] dt \quad (23)$$

This result also extends to conditional diffusion models, where the likelihood of \mathbf{x} given condition \mathbf{y} (e.g., text embeddings) is given by:

$$-\log p(\mathbf{x}|\mathbf{y}) = \frac{1}{2} \int_0^T \lambda(t) \mathbb{E}_{t, \epsilon} [\|\epsilon_\theta(\mathbf{x}_t, t, \mathbf{y}) - \epsilon\|^2] dt \quad (24)$$

B. Implementation Details

The training implementation details are shown in Tab. 3. For Stable diffusion 3, the length of soft token as 4 and the number of layers as 5 are used for the experiments. For Stable diffusion 1.5 and Stable diffusion XL, we used the length of soft token as 8. Soft tokens are added to the original embedding only on the Down and Middle block layers of UNet. Since we found that the performance of the Stable Diffusion 1.5 degrades when soft tokens are initialized with a random distribution. Therefore, unconditional text embedding was utilized for initializing soft tokens.

In Stable diffusion 3, we optimize the soft tokens only using the contrastive score matching loss (L_{SoftREPA}). In Stable diffusion 1.5 and Stable diffusion XL, we optimize the soft tokens with the combination of the contrastive score matching loss function (L_{SoftREPA}) and the small weight of denoising score matching loss. The code is available at <https://github.com/softrepa/SoftREPA>.

Models	lr	wd	batch size	iterations	token init	optimizer	lr scheduler
SD1.5	1e-3	1e-4	16	26,000	\emptyset	AdamW	CosineAnnealingWarmRestarts
SDXL	1e-3	1e-4	16	30,000	$N(0, 0.02)$	AdamW	CosineAnnealingWarmRestarts
SD3	1e-3	1e-4	16	30,000	$N(0, 0.02)$	AdamW	CosineAnnealingWarmRestarts

Table 3. The implementation details for training.

C. Prompt for Editing dataset

To generate source/target text prompt from images, we leverage LLaVA [19]¹ and Llama [8]² sequentially. Specifically, we extract source text description from 800 training images of DIV2K dataset by giving each image and following text prompt to LLaVA.

”Describe the object and background in the image”

¹We use checkpoint from 4bit/llava-v1.5-13b-3GB

²We use Llama-3.1-8B-Instruct model.

Then, we generate the target text prompt that has only a single different concept compared with the source text prompt using Llama with the following instruction.

”You are an AI assistant for generating paired text prompts for real image editing tasks. Your goal is to modify a given text description by replacing an object with other while strictly following these rules:

- 1) Modify only one object (i.e., a single meaningful concept such as an object). It could be small object.
- 2) The replacement must be significantly different from the original concept but contextually appropriate. Avoid unrealistic substitutions (e.g., changing ”rabbit on grass” to ”rocket on grass”).
- 3) Ensure diversity in word choices across different modifications.
- 4) Preserve all other words exactly as they are. Do not change sentence structure, introduce new elements, or modify additional details.
- 5) Do not provide any additional words—output only the modified text description.
- 6) Do not change or add colors. Specifically, when modifying a building, change only the appearance, not the type of building (e.g., do not change ”building” to ”church” or ”lighthouse”).
- 7) Modify only one feature at a time. If changing an object (e.g., ”starfish” to ”sea turtle”), do not alter its color, shape, or other attributes.

Example:

Input: The image features a close-up of a brown dog with a blue nose. The dog is standing in a grassy field, and the background is blurred, creating a focus on the dog’s face. The dog’s ears are perked up, and its eyes are open, giving it a curious and attentive expression. The dog’s fur is brown, and the grass in the background is green, creating a natural and vibrant scene.

Output: The image features a close-up of a brown fox with a blue nose. The fox is standing in a grassy field, and the background is blurred, creating a focus on the fox’s face. The fox’s ears are perked up, and its eyes are open, giving it a curious and attentive expression. The fox’s fur is brown, and the grass in the background is green, creating a natural and vibrant scene.”

D. Additional Results on T2I Generation

The overall quantitative results are shown in Tab. 4. The additional qualitative results on SD1.5 and SDXL are shown in Fig. 8 and Fig. 9

Model	NFE	CFG	Human Preference		Text Alignment		Image Quality	
			ImageReward↑	PickScore↑	CLIP↑	HPS↑	FID↓	LPIPS↓
SD1.5	30	7.0	0.177	21.478	0.264	0.250	24.598	0.438
SD1.5 +Ours	30	7.0	0.273	21.541	0.270	0.252	25.358	0.437
SDXL	30	7.0	0.750	22.389	0.267	0.273	24.697	0.420
SDXL +Ours	30	7.0	0.852	22.620	0.268	0.283	26.040	0.423
SD3	28	4.0	0.942	22.549	0.263	0.280	31.595	0.424
SD3 +Ours	28	4.0	1.085	22.550	0.269	0.289	36.214	0.428

Table 4. Quantitative results of text to image generation on SD1.5, SDXL, and SD3.

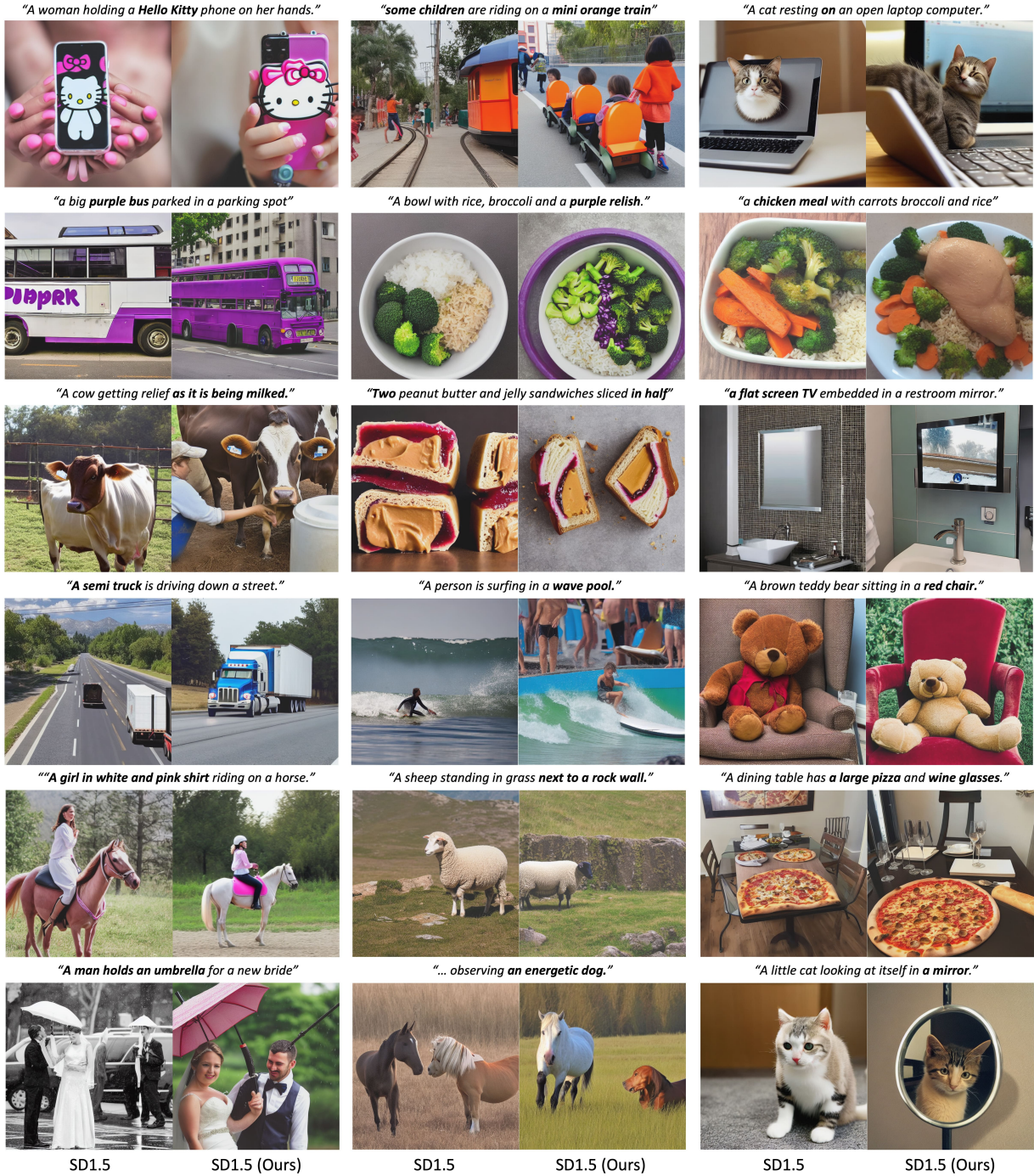


Figure 8. The qualitative results of text-to-image generation comparing SD1.5 and SD1.5 with proposed method. The given text is from COCO and Pixart dataset.

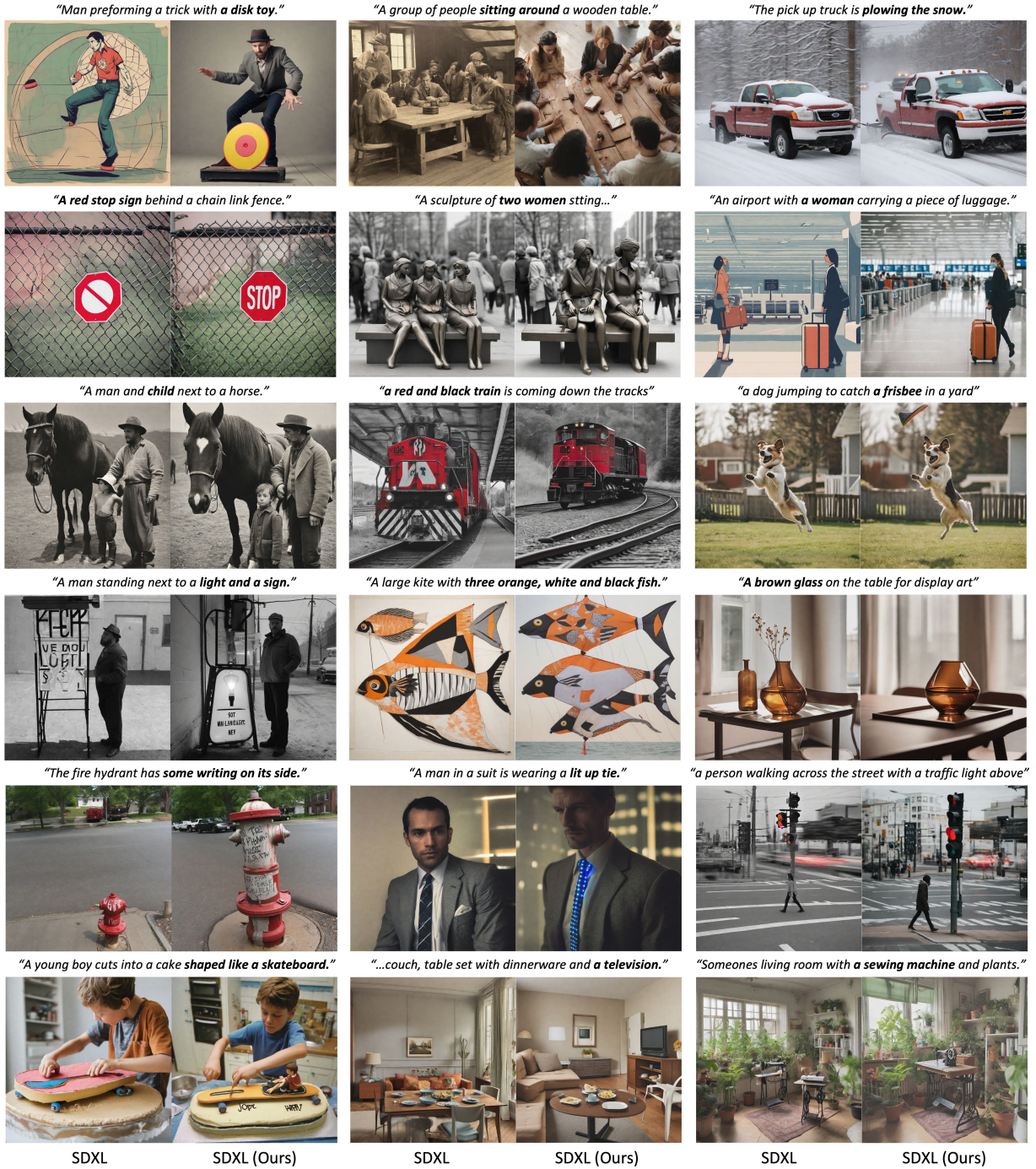


Figure 9. The qualitative results of text-to-image generation comparing SDXL and SDXL with proposed method. The given text is from COCO and Pixart dataset.

E. Additional Results on Image Editing

The overall quantitative results of DIV2K and Cat2Dog dataset on different target CFG scale are shown in Tab. 5 and Tab. 6, respectively. Additionally, qualitative results on different target CFG scale are shown in Tab. 5. The additional qualitative results across different number of editing steps are shown in Fig. 10

Model	NMAX	target CFG	Human Preference		Text Alignment		Image Quality	
			ImageReward↑	PickScore↑	CLIP↑	HPS↑	FID↓	LPIPS↓
FlowEdit	33	13.5	0.380	21.749	0.261	0.255	52.038	0.154
FlowEdit	33	16.5	0.466	21.824	0.263	0.259	55.371	0.180
FlowEdit	33	19.5	0.510	21.869	0.265	0.261	58.069	0.200
FlowEdit +Ours	30	9	0.466	21.884	0.263	0.260	52.633	0.149
FlowEdit +Ours	30	11	0.564	21.985	0.268	0.265	56.900	0.178
FlowEdit +Ours	30	13	0.627	22.050	0.272	0.270	59.710	0.201

Table 5. Quantitative results of image editing regarding image quality and target text alignment of generated images with various target CFG scales on DIV2K dataset.

Model	NMAX	target CFG	Human Preference		Text Alignment		Image Quality	
			ImageReward↑	PickScore↑	CLIP↑	HPS↑	FID↓	LPIPS↓
FlowEdit	33	13.5	0.937	20.726	0.225	0.266	197.1	0.199
FlowEdit	33	16.5	0.908	20.641	0.229	0.272	201.05	0.217
FlowEdit	33	19.5	0.882	20.572	0.232	0.276	202.92	0.234
FlowEdit +Ours	30	7	1.111	21.143	0.226	0.269	198.71	0.173
FlowEdit +Ours	30	9	1.144	21.221	0.234	0.283	208.18	0.204
FlowEdit +Ours	30	11	1.144	21.224	0.239	0.290	214.72	0.230
FlowEdit +Ours	30	13	1.135	21.200	0.241	0.293	219.35	0.252

Table 6. Quantitative results of image editing regarding image quality and target text alignment of generated images with various target CFG scales on Cat2Dog dataset.

F. Additional Results on Ablation Study

The overall quantitative results on different number of layers and number of tokens are shown in Tab. 7. Additionally, qualitative results are shown in Fig. 11 and Fig. 12, respectively. The qualitative results show that the text prompts are emphasized as more layers adopt soft tokens(Fig. 11). The same image of the ablation on the number of tokens are shown in Fig. 12.

# of tokens	# of layers	Human Preference		Text Alignment		Image Quality	
		ImageReward↑	PickScore↑	CLIP↑	HPS↑	FID↓	LPIPS↓
8	2	0.993	22.556	0.263	0.255	72.253	0.428
8	4	1.009	22.464	0.266	0.255	72.308	0.424
8	6	0.984	22.403	0.267	0.255	73.840	0.427
8	7	0.944	22.197	0.269	0.255	74.546	0.425
1	5	1.054	22.492	0.272	0.283	58.430	0.426
4	5	1.063	22.493	0.269	0.287	60.766	0.429
8	5	1.056	22.516	0.268	0.288	62.644	0.431
16	5	0.801	22.095	0.265	0.278	60.743	0.431
32	5	0.675	21.876	0.257	0.275	61.623	0.426

Table 7. Quantitative results of image generation ablation study on the number of soft tokens and the number of layers.

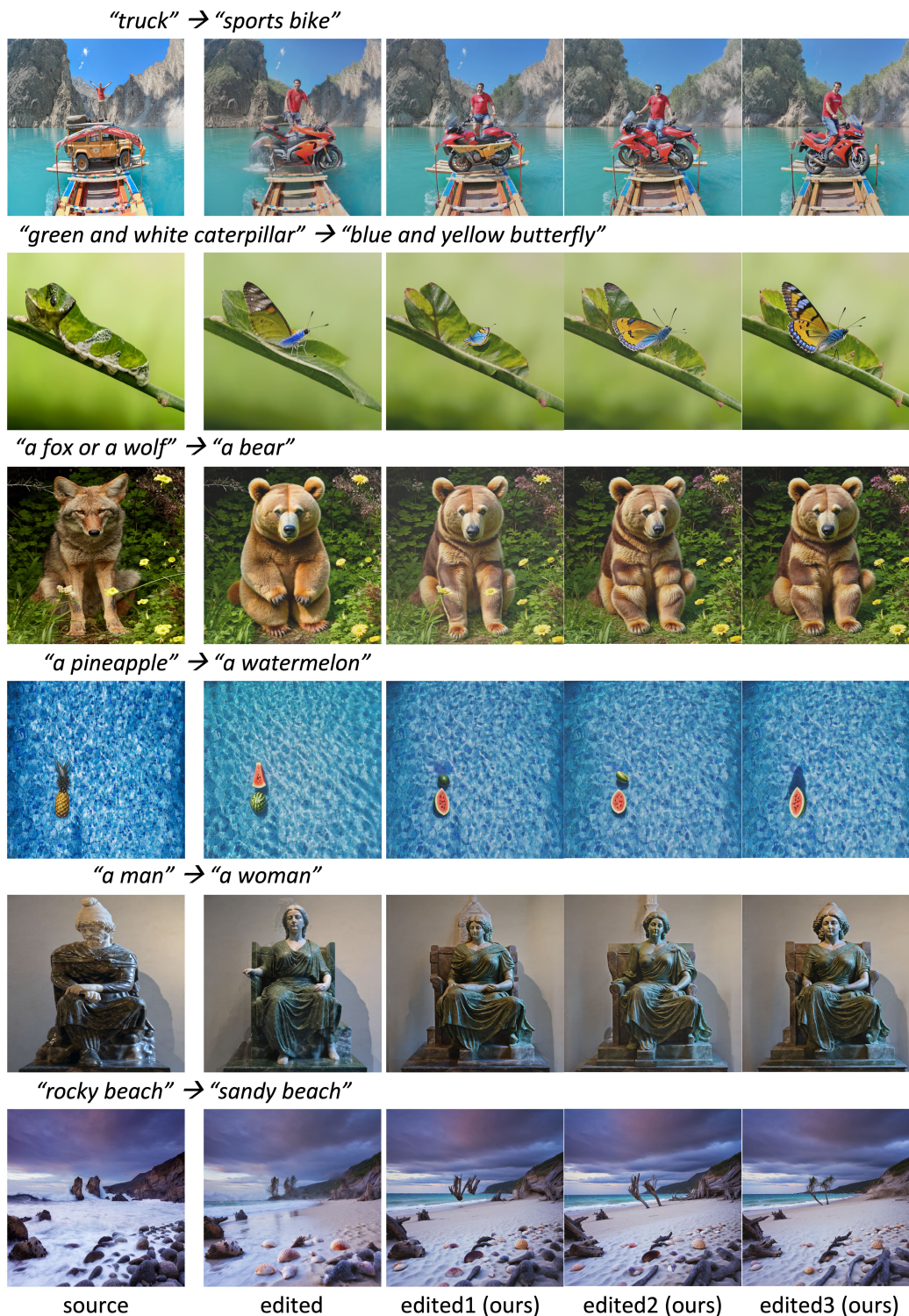
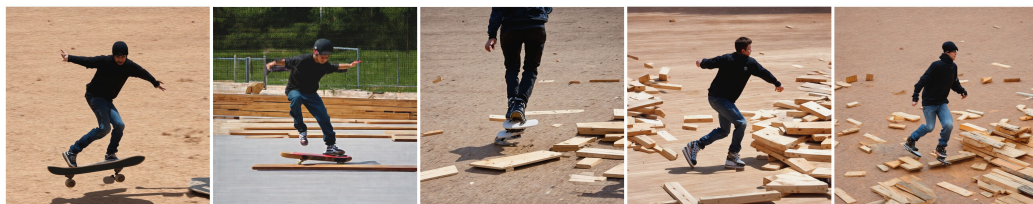


Figure 10. The additional qualitative results on editing using FlowEdit. The three different results adopting soft tokens (edited1-3) are vary on the number of editing steps, 27, 29, 30 out of 50 total timesteps, respectively.

"A person skating on some pieces of wood."



"A shower curtain sits open in an empty and clean bathroom."



"A collection of apples growing on a tree"



"A man is loading luggage suitcases onto the cart in the parking lot."



"A white clock tower at the top of a tiled building."



"A desk top with a bunch of electronics on it."



Text

baseline

Layer #1-2

Layer #1-4

Layer #1-6

Layer #1-7

Figure 11. Qualitative results of the ablation study on **the number of layers** adopting soft tokens.



Figure 12. Qualitative results of the ablation study on **the number of tokens** adopting soft tokens.